

Applications of Bifurcation Methods to F-18/HARV Open-loop Dynamics in Landing Configuration

Nandan Kumar Sinha

Indian Institute of Technology Bombay, Mumbai – 400 076

ABSTRACT

Over the past two decades, bifurcation and continuation methods have emerged as efficient tools for prediction, and control of flight instabilities. Bifurcation phenomena have been associated with nonlinear behaviour of aircraft in actual flight tests, and the critical control combinations, which signify onset of instabilities, have been identified for almost all generations of modern fighter aircraft. A standard bifurcation analysis procedure has been used in the past. In this paper, the bifurcation theory, relevant to preliminary bifurcation analysis of nonlinear aircraft dynamics, has been introduced, and a stepwise methodology used in a standard bifurcation analysis procedure has been illustrated with an application to open-loop dynamics of an F-18/HARV model in landing configuration. Further, an example manoeuvre is constructed, and numerical time simulations of an F-18/HARV model in this manoeuvre is carried out to validate the predictions from the bifurcation analysis. Numerical time simulation results confirm the onset of nonlinear behaviour at critical control combinations identified in bifurcation analysis of the aircraft model. Thus, bifurcation methods, in conjunction with selective numerical simulations, can be extremely useful in the design, development, evaluation, and flight training phases of a fighter aircraft development programme.

Keywords: Bifurcation methods, standard bifurcation analysis, open-loop dynamics, flight control, flight instabilities, nonlinear aircraft dynamics, nonlinear dynamics, flight mechanics, fighter aircraft, aircraft instabilities prediction, wing rock motion

NOMENCLATURE

		p, q, r	Body axis roll, pitch, and yaw rates
b	Wing span	S	Wing planform area
c	Mean wing chord	t	Time
C_D, C_Y, C_L	Drag, sideforce, and lift coefficients	T_m	Maximum thrust
C_p, C_m, C_n	Roll, pitch, and yaw moment coefficients	v_s	Speed of sound
g	Gravitational acceleration	α, β	Angles of attack and sideslip
I_x, I_y, I_z	Inertia about aircraft X, Y, and Z axes	γ, μ	Wind axis pitch and roll Euler angles
M	Mach number	$\delta e, \delta a, \delta r$	Elevator, aileron, and rudder deflections
m	Aircraft mass	η	Throttle, as fraction of maximum thrust

ϕ, θ	Body axis roll and pitch Euler angles
ρ	Atmospheric density at sea level conditions
w	Frequency of limit cycle oscillation

Subscripts

cr	Critical equilibrium point
T	T -periodic solution
0	Equilibrium point

1. INTRODUCTION

Modern combat aircraft are being designed for controlled flights at high angles of attack and in rapid roll manoeuvres. However, high manoeuvrability is often achieved at the risk of losing flight stability. It is known that aircraft, in high angles of attack motion and in rapid roll manoeuvres, may undergo nonlinear transitions, such as jump between two rival equilibrium states, and transition from equilibrium to periodic motion (so-called limit cycle oscillation) in flights as controls are varied. Therefore, studying nonlinear phenomena, and prediction and control of various instabilities has always been one of the problems of major interest in flight dynamics.

Carroll and Mehra¹, and Zagaynov and Goman² introduced bifurcation and continuation theory-based methods as efficient tools for investigating nonlinear aircraft dynamics. Using bifurcation analysis methods, they predicted a variety of nonlinear phenomena occurring in flights, and associated each of these with bifurcation phenomena. For example, wing rock motion was related to a Hopf bifurcation, and jump was found to be the result of a saddle-node bifurcation of equilibrium solutions. Carroll and Mehra also calculated steady spin modes of an aircraft. Thus, they were able to predict both the control surface deflections at which the aircraft would undergo stall/spin divergence, and the resulting steady states of the aircraft. Since then, bifurcation analysis methods have become a standard tool for studying nonlinear aircraft dynamics. Some

interesting studies pertaining to applications of bifurcation methods to nonlinear aircraft dynamics are available in literature³⁻⁶.

Results based on bifurcation methods have also been used as reference maps for control law design. Ananthkrishnan and Sudhakar⁷ used bifurcation methods to design a linear aileron-rudder interconnect law to prevent jump phenomena occurring in roll manoeuvres of an aircraft. Lowenberg⁸ proposed a bifurcation tailoring approach, where multiple control actuators could be scheduled to avoid undesirable dynamic behaviour like spin. Use of bifurcation methods in the aircraft design and development process has also been stressed upon by Lowenberg⁹, and most recently by Liaw and Song¹⁰. Therefore, one can say that bifurcation theory-based methodology is becoming a powerful tool in nonlinear flight dynamics.

This paper aims to provide readers with an introduction to the bifurcation theory and to illustrate the standard bifurcation analysis procedure with an application to study the open-loop dynamics of an F-18/HARV model¹¹ in landing configuration, and to validate the predictions from the bifurcation analysis of an F-18/HARV model with numerical simulation results. For bifurcation analysis, AUTO97 continuation algorithm¹² has been used, and all numerical simulation results have been produced on MATLAB.

2. BIFURCATION THEORY

In a bifurcation analysis, a dynamical system such as that for the dynamics of a rigid aircraft, is required to be represented by a set of first-order autonomous ordinary differential equations as

$$\dot{x} = f(x, u, p) \quad (1)$$

where x is the vector of n state variables of the system, u is the varying control parameter, p is the vector of fixed control parameter, and f is the vector of nonlinear functions which includes the effects of aerodynamics, thrust, and gravity. In an analysis using bifurcation methods, it is of interest to solve for all possible asymptotic states as u is varied within the prescribed limits, while p are

always kept fixed at their starting values. For a fixed value of $u = u_0$, two types of asymptotic states are commonly encountered: Steady state or equilibrium solution, denoted by $x = x_0$ at $\bar{u} = u_0$, and (ii) periodic solution, $x_T(t + T) = x_T(t)$ at $u = u_0$, where T is the time period of the periodic solution.

2.1 Stability of Asymptotic States

Stability of an asymptotic state is computed by local linearisation of the system about the asymptotic state under consideration and is based on Lyapunov's and Poincare's definitions of stability¹³.

2.1.1 Stability of Equilibrium Solutions

The locally linearised system around an equilibrium solution is represented by the Jacobian matrix, $J = \partial f / \partial x$. Practically, stability of an equilibrium solution is decided by the eigenvalues of the Jacobian matrix, evaluated at the equilibrium solution under consideration. The condition for local asymptotic stability of the system at that equilibrium solution is that all the eigenvalues of J lie in the left half complex plane. One or more eigenvalues in the right half complex plane indicate an unstable steady state. A critical or non-hyperbolic¹³ equilibrium state is the one which has one or more eigenvalues lying on the imaginary axis, i.e., eigenvalues with a zero real part. The linearised stability criterion is not applicable to critical equilibrium states. Stability of a critical equilibrium state depends on the higher order terms ($\partial^2 f / \partial x^2$, $\partial^3 f / \partial x^3$, etc.) in the Taylor series expansion of the system about the equilibrium point.

2.1.2 Stability of Periodic Solutions

The locally linearised system around a periodic solution is represented by $\delta \dot{x} = A(t) \delta x$, where $\delta x(t) = x(t) - x_T(t)$ is a small perturbation from the periodic solution $x_T(t)$, and $A(t)$ is a square $n \times n$ T -periodic matrix. $A(t)$ can be transformed to a matrix known as the monodromy matrix¹⁴. Eigenvalues of the monodromy matrix, known as Floquet multipliers, are used to indicate

stability of the periodic solution. One of the Floquet multipliers is necessarily unity, the other $(n - 1)$ must lie within the unit circle in the complex plane for stability¹⁵.

2.2 Local Bifurcations of Asymptotic States

As stated earlier, in a bifurcation analysis, it is necessary to solve for all asymptotic states of the system as the control parameter u is varied. This is best done using a continuation algorithm. Locations where the number and/or stability of equilibrium or periodic solutions change are called bifurcation points. Bifurcations that are based on the knowledge of local behaviour of equilibrium points, are called local bifurcations to distinguish them from global bifurcations¹⁵.

2.2.1 Local Bifurcations of Equilibrium Solutions

There are two types of bifurcations: (i) static bifurcations arise when branches of equilibrium solutions meet at a point, and (ii) merging of periodic solutions and stationary solutions at a point is called dynamic or Hopf bifurcation.

2.2.1.1 Static Bifurcations

In the $x - u$ state-parameter space, a static bifurcation of equilibrium solutions of Eqn (1) occurs at (x_{cr}, u_{cr}) , if the following conditions are satisfied:

- $f(x_{cr}, u_{cr}) = 0$
- Jacobian matrix (J) evaluated at (x_{cr}, u_{cr}) has a zero eigenvalue, while all of its other eigenvalues have non-zero real parts, i.e., $\text{rank}(J) = n - 1$.

The first condition ensures that the considered solution is an equilibrium solution or fixed point of Eqn (1), and the second condition implies that this fixed point is a non-hyperbolic or critical fixed point. There are three types of static bifurcations¹³ [Figs 1(a) – 1(c)]: (i) saddle-node, (ii) pitchfork, and (iii) transcritical. These are structurally different and have different

non-hyperbolic or critical fixed point. When all the above conditions are satisfied, a periodic solution of period $2\pi/\omega$ is born at (x_{cr}, u_{cr}) . The Hopf bifurcation point, and the branching of a single stable equilibrium solution branch into an unstable equilibrium solution branch, and a stable periodic solution branch is shown in Fig.1(d).

2.2.2 Local Bifurcations of Periodic Solutions

Periodic solutions can also undergo an exchange of stability¹⁵. Analogous to local bifurcations of equilibrium solutions which depend on the location of eigenvalues in the complex plane, local bifurcations of periodic solutions are characterised by the location of Floquet multipliers on a unit circle in the complex plane.

2.3 Continuation Algorithms

Continuation algorithms, used to compute branches of equilibrium and periodic solutions, are based on the implicit function theorem¹⁶. Continuation algorithm available in the public domain¹² is AUTO97*. It can compute branches of equilibrium points, periodic solutions, and also it can locate folds, period/doubling bifurcations, etc. Type of each bifurcation point is also determined. Starting data for computations is generally an equilibrium point. At Hopf bifurcation points, AUTO97¹² generates starting data to compute periodic orbits. These can then be used as starting points to compute bifurcations from periodic orbits.

3. BIFURCATION ANALYSIS OF AN F-18/HARV MODEL

The aircraft model (*Appendix A*) is in the required form, $\dot{x} = f(x, u, p)$, suitable for implementing bifurcation methods to study its dynamics. One can identify from a comparison of the aircraft model (*Appendix A*) with the general model of a nonlinear system [Eqn (1)] that, $x = [M, \alpha, \beta, p, q, r, \phi, \theta]$, and a typical choice of u and p for the pre sent analysis is, $u = \delta e$, and $p = [\eta, \delta a, \delta r]$.

3.1 Steady State Continuation

This is the first step in a standard bifurcation analysis. In this step, a continuation algorithm is used to compute all possible steady states of the system as the control parameter u is varied within the prescribed limits. To begin with the continuation, a starting equilibrium point is needed, which can either be obtained using analytical methods or by numerical simulations of the model. For the present analysis, the starting equilibrium point is a level flight trim:

$$\begin{aligned} x_0 &= [M_0, \alpha_0, \beta_0, p_0, q_0, r_0, \phi_0, \theta_0] \\ &= [0.28, 0.03, 0, 0, 0, 0, 0, 0.03] \\ u_0 &= [\delta e_0 = -0.1745] \\ p_0 &= [\eta_0 = 0.569, \delta a_0 = 0, \delta r_0 = 0] \end{aligned}$$

where all angles are in radian and angular rates are in radian per second. Starting with this equilibrium point, the AUTO97 continuation algorithm was used to compute other steady states of the model (*Appendix A*) as elevator deflection varied within the prescribed limits. The throttle parameter η , aileron deflection δa , and rudder deflection δr were always kept fixed in this continuation at their starting values as given above. The steady states, so computed, are plotted in Fig. 2 as functions of δe . Plots in Fig. 2 are popularly known as bifurcation diagrams.

3.2 Interpretation of Bifurcation Diagrams & Instability Prediction

On the bifurcation diagrams plotted in Fig. 2, solutions represented by solid lines are stable trims, and those represented by dashed lines are unstable trims. Onset of instability is represented by a bifurcation point. Between the bifurcation points at $\alpha \approx 0.4$ rad and $\alpha \approx 0.08$ rad, represented by solid square and empty square respectively, lies the region of stable longitudinal trims, as the lateral state variables, (p, β, ϕ, r) are all zero in this region. The longitudinal trims in this region comprise three different phases of longitudinal flight, viz., level, ascent, and descent. This is quite expected as the throttle η , which is also the thrust available, has been kept fixed in this

*AUTO97 can be downloaded from the website ftp.cs.concordia.ca.

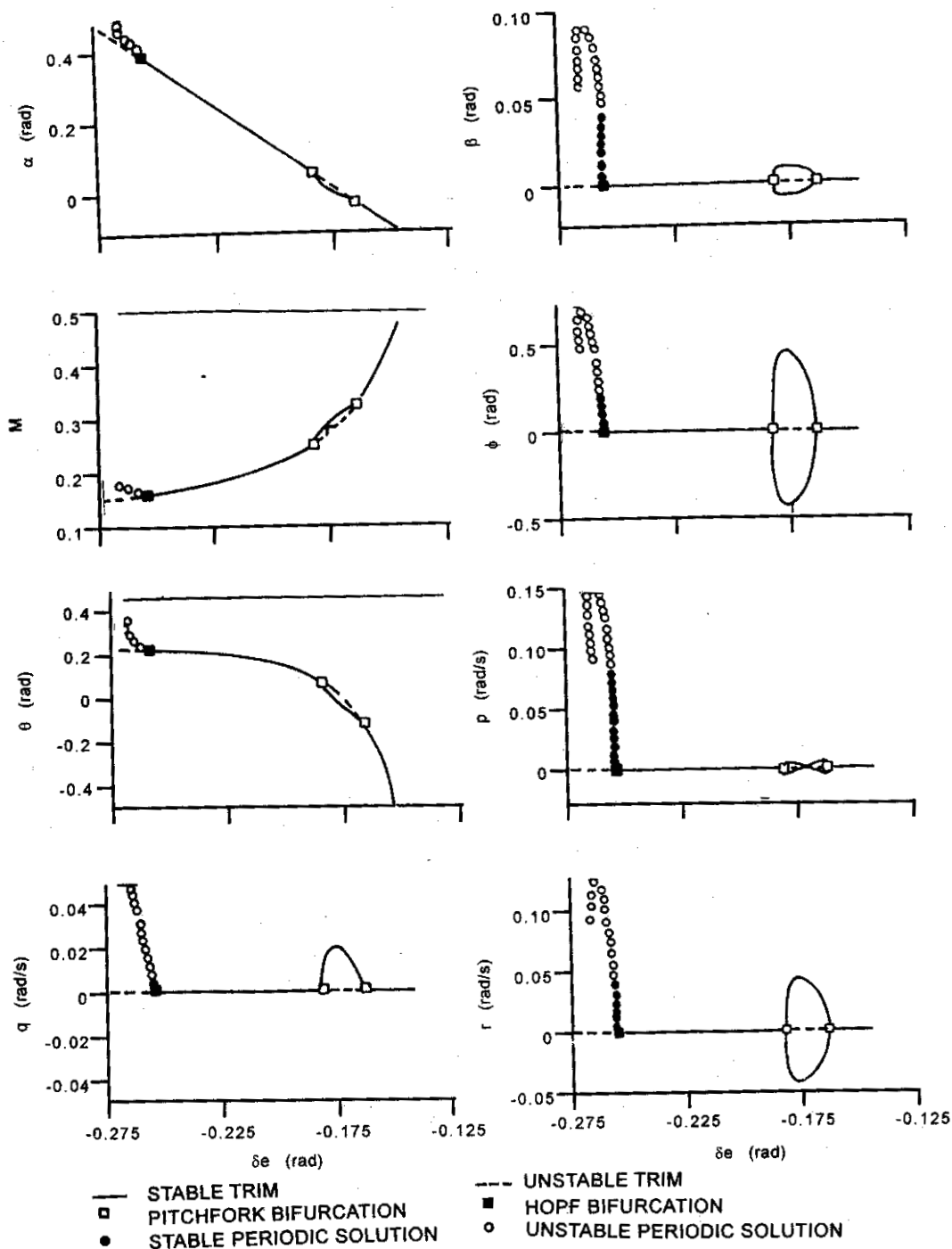


Figure 2. Bifurcation diagrams for F-18/HARV open-loop dynamics as a function of elevator deflection δ_e

analysis, and elevator is the only control being varied. Different trim values of the elevator deflection bring the aircraft into different phases of flight depending on the amount of

lift and drag generated. The three phases of the longitudinal flight are characterised by the flight path angle, $\gamma = (\theta - \alpha)$, and from an inspection of α and q values in Fig. 2, one can easily

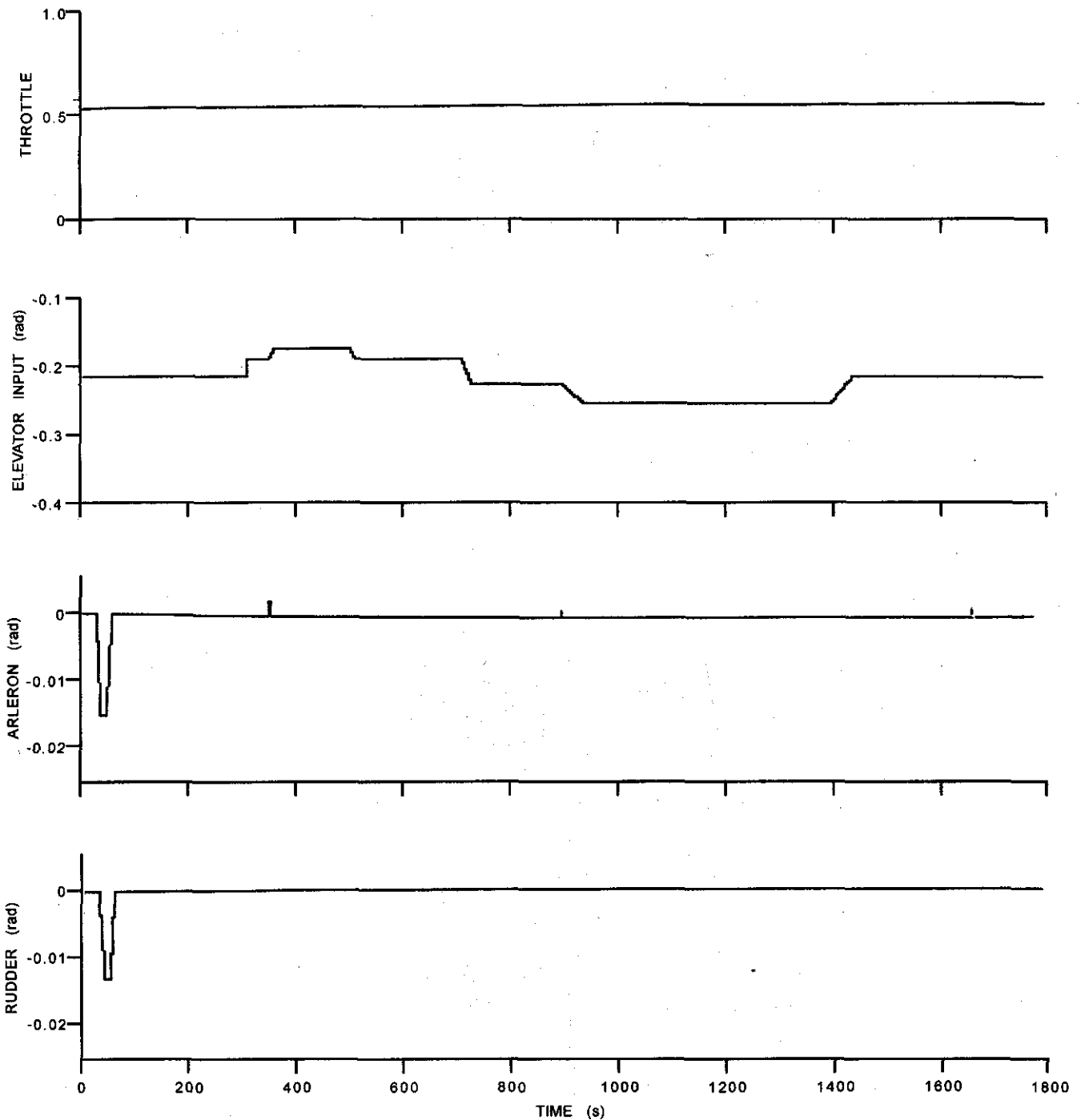


Figure 3. Control inputs for manoeuvre

identify these on the bifurcation diagrams. At $\alpha \approx 0.4$ rad, which is a descending trim ($\gamma < 0$) inflight, the aircraft encounters a Hopf bifurcation point, which in bifurcation theory (as observed from [Fig. 1(d)] is the onset of limit cycling motion. As the longitudinal trims are unstable beyond

the Hopf bifurcation point, it is predicted that the aircraft will undergo limit cycle oscillations. Also, as this instability is found to be due to the Dutch roll mode eigenvalues, this limit cycling motion is predicted to be wing rock. In the ascending phase ($0.03 \text{ rad} < \alpha < 0.25 \text{ rad}$) of

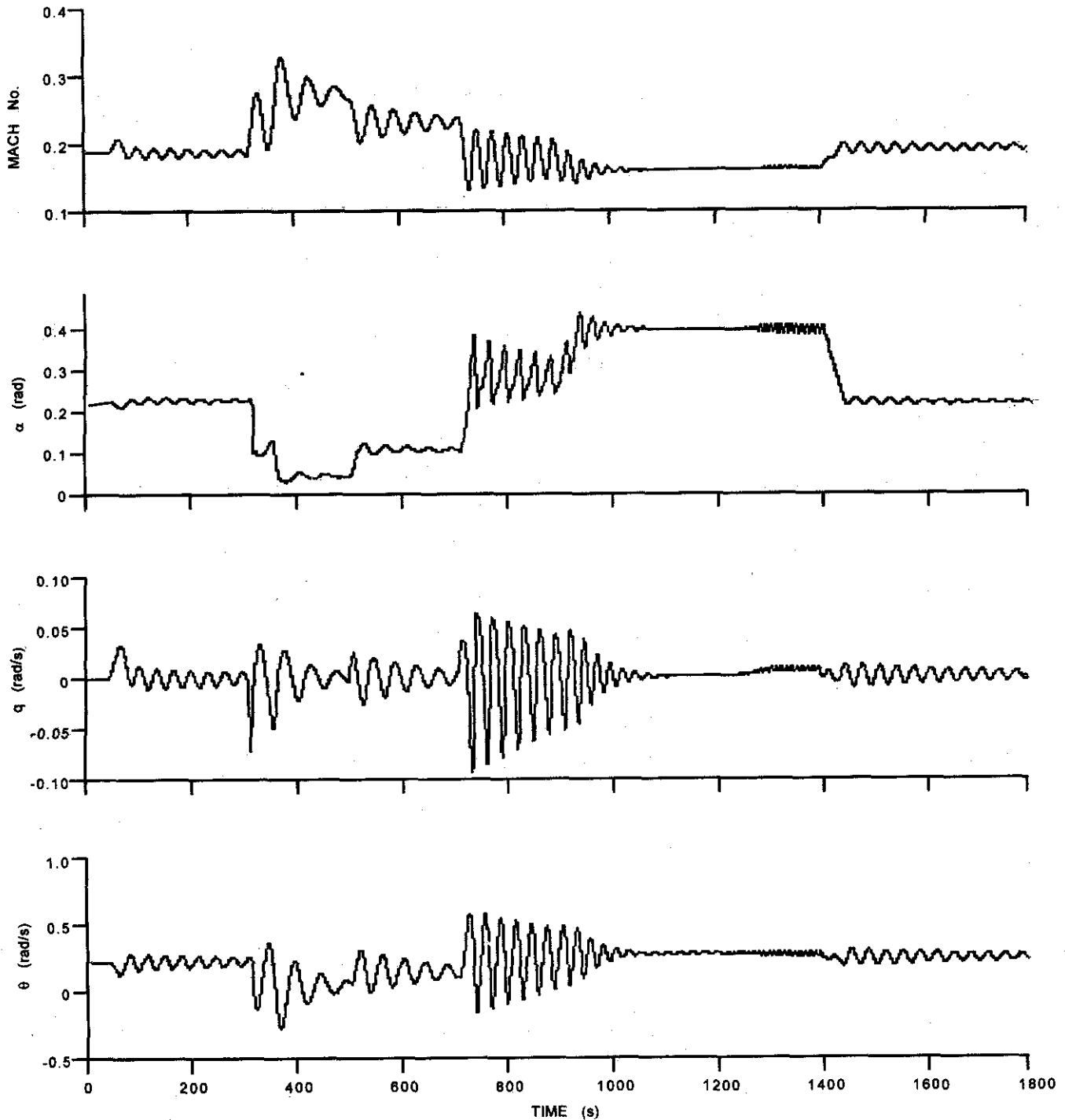


Figure 4. Transient response of longitudinal state variables of aircraft in manoeuvre

flight, as elevator is deflected down, α decreases, flight path angle γ decreases, and the aircraft is encountered with a branch point at $\alpha \approx 0.08$ rad. One can identify from the basic bifurcation diagram [Fig. 1(b)] that this branch point

corresponds to a pitchfork bifurcation. Below this point lies the region of unstable longitudinal trim flight, and bifurcated stable solution branch with non-zero values of lateral state variables. As the pitchfork bifurcation point was due to

the spiral mode eigenvalue of the aircraft, it is predicted that the stable solution branch with non-zero values of the lateral state variables corresponds to the coupled dynamics of the aircraft, which is the spirally divergent motion of the aircraft. The peak on the spirally divergent solution branch is marked by a level trim flight ($\gamma = 0$) condition at $\alpha = 0.03$ rad, below which aircraft starts descending. On this descending phase of flight, spiral mode eigenvalue of the aircraft again moves into the left half complex plane at $\alpha = -0.02$ rad, below which, the descending phase of flight is represented by stable longitudinal trims.

3.3 Validation of Predictions

This step must be carried out to confirm the predictions based on bifurcation analysis with numerical time simulation results. A practical situation was taken to confirm the predictions based on bifurcation analysis by numerically simulating a manoeuvre of the F-18/HARV model. Description of the manoeuvre is as follows: Starting from a level flight trim condition the aircraft is banked and consequently yawed by applying aileron and rudder so that it is heading in the opposite direction (π rad yaw). At the moment when heading has been achieved, aileron and rudder are brought back to neutral to level out wings. Next, to confirm the presence of instabilities, as identified on the bifurcation diagrams, the aircraft is flown on longitudinal flight trims in the opposite heading attitude. After confirming the presence of instabilities, the aircraft is flown back to the starting level flight condition while maintaining its heading in the opposite direction. On the longitudinal flight of the aircraft, only elevator is operated while keeping other controls at their fixed values, as done in the bifurcation analysis. Control inputs deployed to execute this manoeuvre are shown in Fig.3, and the simulation results are presented in Figs 4 and 5 for longitudinal and lateral state variables, respectively. These numerical simulation results confirm the onset of spiral divergence at $\alpha = 0.08$ rad, and wing rock instability at $\alpha = 0.4$ rad, as predicted by the bifurcation

analysis of the model. Onset of wing rock motion characterised by limit cycle oscillations dominated by lateral state variables of the aircraft can be observed (Fig. 5) when elevator is deflected to $\delta e = -0.257$ rad corresponding to $\alpha = 0.4$ rad. Spirally divergent motions of the aircraft starting at $\alpha = 0.08$ rad, though not clearly visible in other lateral state variables because of their low magnitudes, can be observed in yaw angle response (Fig. 5) where yaw angle changes significantly in response to a 2s step aileron input introduced as a perturbation. Recovery from the wing rock motion is achieved by changing the elevator deflection in downward direction, and it can be observed from Figs 4 and 5 that the aircraft has been brought back to the initial level flight condition, while maintaining the heading angle at approximately π rad.

4. CONCLUSION

Nonlinear behaviour of fighter aircraft at high angles of attack is complex due to its nonlinear aerodynamics, and it is, in general, difficult to predict aircraft behaviour in these regimes accurately. Investigation of this flight domain is usually carried out with exhaustive numerical simulations before the first flight has taken, and later on, by means of expensive and extensive flight testings. Bifurcation and continuation methods, however, provide an efficient and economical way for the analysis of nonlinear behaviour of aircraft and prediction of aircraft instabilities. Efficiency of the method makes it possible to analyse complicated nonlinear aerodynamic models using the complete equations of motion in the entire range of control surface deflections. With little time and effort, global stability information of the nonlinear behavior of aircraft is obtained. Critical control deflections that signify onset of instabilities are easily identified on bifurcation diagrams, and nonlinear behaviour of aircraft are accurately predicted. Selective numerical simulations around bifurcation points confirm the predictions based on bifurcation results. The critical control deflections could be used to define the boundary for safe flight, and can serve as warning signals for the pilot approaching the boundary in flight tests. For

the spiral mode eigenvalue of the aircraft, it is predicted that the stable solution branch with non-zero values of the lateral state variables corresponds to the coupled dynamics of the aircraft, which is the spirally divergent motion of the aircraft. The peak on the spirally divergent solution branch is marked by a level trim flight ($\gamma = 0$) condition at $\alpha = 0.03$ rad, below which aircraft starts descending. On this descending phase of flight, spiral mode eigenvalue of the aircraft again moves into the left half complex plane at $\alpha = -0.02$ rad, below which, the descending phase of flight is represented by stable longitudinal trims.

3.3 Validation of Predictions

This step must be carried out to confirm the predictions based on bifurcation analysis with numerical time simulation results. A practical situation was taken to confirm the predictions based on bifurcation analysis by numerically simulating a manoeuvre of the F-18/HARV model. Description of the manoeuvre is as follows: Starting from a level flight trim condition the aircraft is banked and consequently yawed by applying aileron and rudder so that it is heading in the opposite direction (π rad yaw). At the moment when heading has been achieved, aileron and rudder are brought back to neutral to level out wings. Next, to confirm the presence of instabilities, as identified on the bifurcation diagrams, the aircraft is flown on longitudinal flight trims in the opposite heading attitude. After confirming the presence of instabilities, the aircraft is flown back to the starting level flight condition while maintaining its heading in the opposite direction. On the longitudinal flight of the aircraft, only elevator is operated while keeping other controls at their fixed values, as done in the bifurcation analysis. Control inputs deployed to execute this manoeuvre are shown in Fig.3, and the simulation results are presented in Figs 4 and 5 for longitudinal and lateral state variables, respectively. These numerical simulation results confirm the onset of spiral divergence at $\alpha = 0.08$ rad, and wing rock instability at $\alpha = 0.4$ rad, as predicted by the bifurcation

analysis of the model. Onset of wing rock motion characterised by limit cycle oscillations dominated by lateral state variables of the aircraft can be observed (Fig. 5) when elevator is deflected to $\delta e = -0.257$ rad corresponding to $\alpha = 0.4$ rad. Spirally divergent motions of the aircraft starting at $\alpha = 0.08$ rad, though not clearly visible in other lateral state variables because of their low magnitudes, can be observed in yaw angle response (Fig. 5) where yaw angle changes significantly in response to a 2s step aileron input introduced as a perturbation. Recovery from the wing rock motion is achieved by changing the elevator deflection in downward direction, and it can be observed from Figs 4 and 5 that the aircraft has been brought back to the initial level flight condition, while maintaining the heading angle at approximately π rad.

4. CONCLUSION

Nonlinear behaviour of fighter aircraft at high angles of attack is complex due to its nonlinear aerodynamics, and it is, in general, difficult to predict aircraft behaviour in these regimes accurately. Investigation of this flight domain is usually carried out with exhaustive numerical simulations before the first flight has taken, and later on, by means of expensive and extensive flight testings. Bifurcation and continuation methods, however, provide an efficient and economical way for the analysis of nonlinear behaviour of aircraft and prediction of aircraft instabilities. Efficiency of the method makes it possible to analyse complicated nonlinear aerodynamic models using the complete equations of motion in the entire range of control surface deflections. With little time and effort, global stability information of the nonlinear behavior of aircraft is obtained. Critical control deflections that signify onset of instabilities are easily identified on bifurcation diagrams, and nonlinear behaviour of aircraft are accurately predicted. Selective numerical simulations around bifurcation points confirm the predictions based on bifurcation results. The critical control deflections could be used to define the boundary for safe flight, and can serve as warning signals for the pilot approaching the boundary in flight tests. For

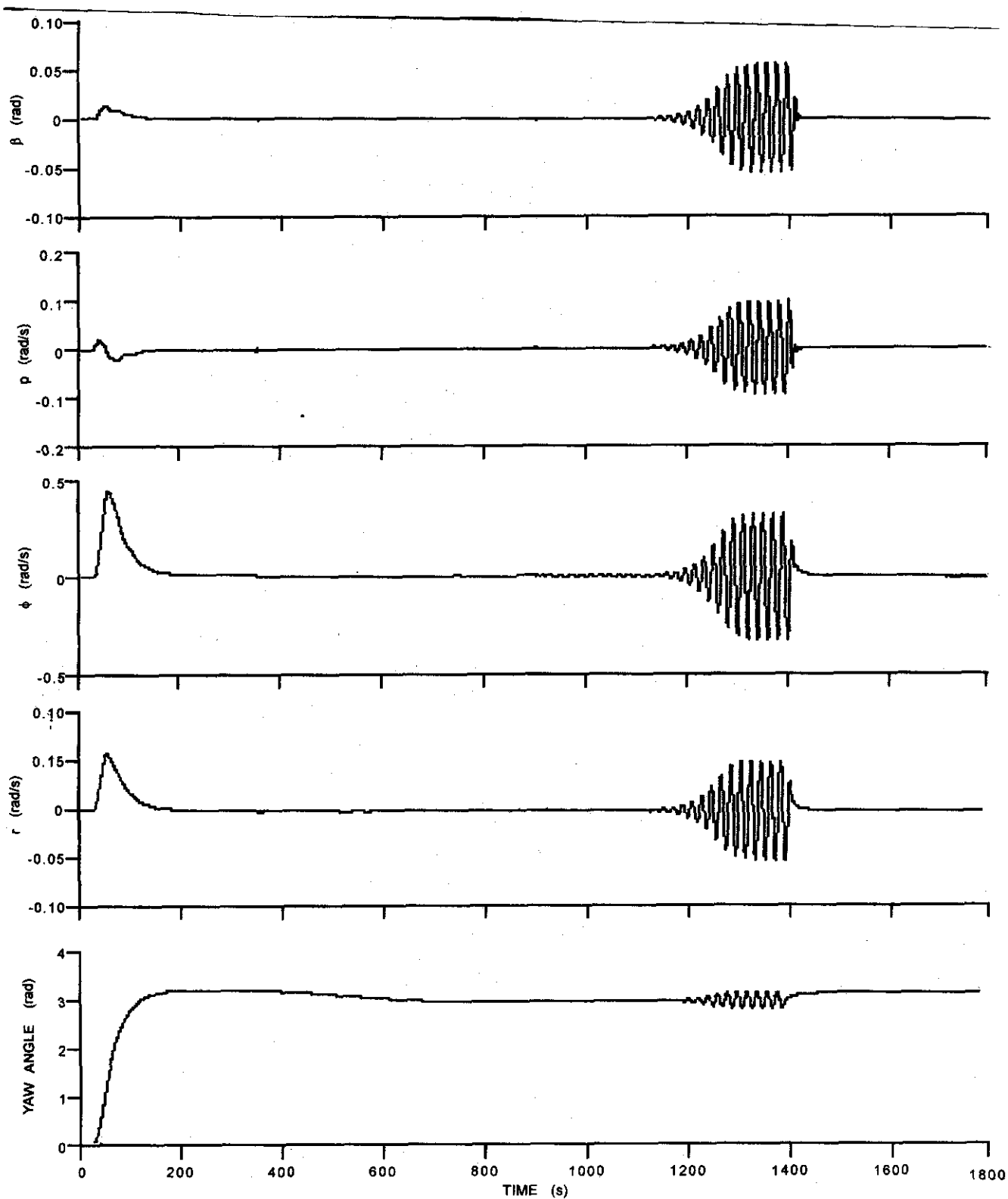


Figure 5. Transient response of lateral state variables of aircraft in manoeuvre

example, presence of Hopf bifurcation point (Fig. 2), which leads to the onset of wing rock motion, can be used as a warning signal for the pilot, so that the pilot stays away from entering into the oscillatory motion.

Results obtained from bifurcation analysis are also important from control point of view, as a bifurcation diagram not only provides the critical control deflection at which unstable motion develops but also provides the mode of instability. Thus, it provides a complete reference map, which could be used as an aid to control law design. For instance, on the bifurcation diagrams (Fig. 2) for the open-loop dynamics of the F-18/HARV model, presence of Hopf bifurcation point was related to the Dutch roll mode eigenvalues of the aircraft, and the branch point was related to the spiral mode eigenvalue. These information could be used to design control laws to stabilise the corresponding modes of the aircraft.

The closed-loop dynamics of the aircraft (with control laws implemented) is expected to have expanded flight envelope with no bifurcation points in the prescribed range of control deflections. Bifurcation analysis procedure does not put any restrictions on the order of the system, additional equations representing actuator dynamics, and flight control systems could also be integrated in the aircraft governing equations of motion and their global effects on the dynamics be studied in a unified manner.

REFERENCES

1. Carroll, J.V. & Mehra, R.K. Bifurcation analysis of nonlinear aircraft dynamics. *J. Guid. Cont. Dyn.*, **5**(5), 1982, 529-36.
2. Zagaynov, G.I. & Goman, M.G. Bifurcation analysis of critical aircraft flight regimes. ICAS84-4.2.1, September 1984, 217-23.
3. Jahnke, C.C. & Culick, F.E.C. Application of bifurcation theory to the high-angle-of-attack dynamics of the F-14. *Journal Aircraft*, **31**(1), 1994, 26-34.
4. Avanzini, G. & de Matteis, G. Bifurcation analysis of a highly augmented aircraft model. *J. Guid. Cont. Dyn.*, **20**(4), 1997, 754-59.
5. Littleboy, D.M. & Smith, P.R. Using bifurcation methods to aid nonlinear dynamic inversion control law design. *J. Guid. Cont. Dyn.*, 1998, **21**(4), 632-38.
6. Goman, M.G.; Zagaynov, G.I. & Khramtsovsky, A.V. Application of bifurcation methods to nonlinear dynamics problems. *Prog. Aerospace Sci.*, 1997, **33**, 539-86.
7. Ananthkrishnan, N. & Sudhakar, K. Prevention of jump in inertia-coupled roll maneuvers of aircraft, *Journal Aircraft*, **31**(4), 1994, 981-83.
8. Lowenberg, M.H. Development of control schedules to modify spin behaviour. American Institute of Aeronautics and Astronautics. AIAA Paper No. 98-4267, 1998, 286-96.
9. Lowenberg, M.H. Bifurcation methods— a practical methodology for implementation by flight dynamicists. ICAS-5.10(R), 1990, 1-11.
10. Liaw, D.C. & Song, C.C. Analysis of longitudinal flight dynamics: A bifurcation-theoretic approach. *J. Guid. Cont. Dyn.*, 2001, **24**(1), 109-16.
11. Fan, Y.; Lutze, F.H. & Cliff, E.M. Time-optimal lateral manoeuvres of an aircraft, *J. Guid., Cont., Dyn.*, 1995, **18**(5), 1106-12.
12. Doedel, E.J.; Wang, X.J.; Fairgrieve, T.F.; Champneys, A.R.; Kuznetsov, Y.A. & Sandstede, B. AUTO 97: Continuation and bifurcation software for ordinary differential equations (with HomCont). California Institute of Technology, Pasadena, CA, 1998.
13. Nayfeh, H. & Balachandran, B. Nonlinear applied dynamics. Springer-Verlag, New York, 1985.
14. Guckenheimer, J. & Holmes, P. Nonlinear oscillations, dynamical systems, and bifurcations of vector fields. Springer-Verlag, New York, 1983.

15. Seydel, R. Practical bifurcation and stability analysis. Springer-Verlag, New York, 1994.
16. Allgower, E.L. & Georg, K. Numerical continuation methods—an introduction. Springer-Verlag, Berlin, 1990.

Contributor

Mr Nandan Kumar Sinha is a research scholar in the Dept of Aerospace Engineering at the Indian Institute of Technology (IIT) Bombay, Mumbai. He received his BTech from IIT Bombay in 1996 and MTech (Aerospace Engineering) from IIT Kanpur in 1998. His areas of specialisation are: Flight mechanics and control, nonlinear dynamics, bifurcation methods, and aerodynamics.

Mathematical Model of Aircraft Dynamics

The governing equations of motion for rigid aircraft dynamics are as follows:

$$\dot{M} = \frac{1}{mv_s} \left[T_m \eta \cos \alpha \cos \beta - \frac{1}{2} C_D(\alpha) \rho (v_s M)^2 S - mg \sin \gamma \right] \quad (2)$$

$$\dot{\alpha} = q - \frac{1}{\cos \beta} \left[(p \cos \alpha + r \sin \alpha) \sin \beta + \frac{1}{mv_s M} (T_m \eta \sin \alpha + \frac{1}{2} C_l(\alpha, \delta e) \rho (v_s M)^2 S - mg \cos \mu \cos \gamma) \right] \quad (3)$$

$$\dot{\beta} = \frac{1}{mv_s M} \left[-T_m \eta \cos \alpha \sin \beta + \frac{1}{2} C_y(\alpha, \beta, \partial a, \partial r) \rho (v_s M)^2 S + mg \sin \mu \cos \gamma \right] + p \sin \alpha - r \cos \alpha \quad (4)$$

$$\dot{p} = \frac{I_y - I_z}{I_x} qr + \frac{1}{2I_x} \rho (v_s M)^2 S b C_1(\alpha, \beta, p, r, \partial a, \partial r) \quad (5)$$

$$\dot{q} = \frac{I_z - I_x}{I_y} pr + \frac{1}{2I_y} \rho (v_s M)^2 S c C_m(\alpha, q, \partial e) \quad (6)$$

$$\dot{r} = \frac{I_x - I_y}{I_z} pq + \frac{1}{2I_z} \rho (v_s M)^2 S b C_n(\alpha, \beta, p, r, \partial a, \partial r) \quad (7)$$

$$\dot{\phi} = p + q \sin \phi \tan \theta + r \cos \phi \tan \theta \quad (8)$$

$$\dot{\theta} = q \cos \phi - r \sin \phi \quad (9)$$

where wind orientation angles μ and γ can be determined from the following equations:

$$\sin \gamma = \cos \alpha \cos \beta \sin \theta - \sin \beta \sin \phi \cos \theta - \sin \alpha \cos \beta \cos \phi \cos \theta$$

$$\sin \mu \cos \gamma = \sin \theta \cos \alpha \sin \beta + \sin \phi \cos \theta \cos \beta - \sin \alpha \sin \beta \cos \phi \cos \theta$$

$$\cos \mu \cos \gamma = \sin \theta \sin \alpha + \cos \alpha \cos \phi \cos \theta$$